Experimental and Numerical Investigation of Air Radiation in Superorbital Expanding Flow

Han Wei [1] Richard G. Morgan [1] Timothy J. McIntyre[1]
Aaron M. Brandis [2] Christopher O. Johnston [3]

[1]Centre for Hypersonics, the University of Queensland

[2]AMA at NASA Ames Research Center

[3]NASA Langley Research Center

9th June 2017

Outline

Outline

Afterbody TPS

Afterbody Heatshield:

- Cocooning the bulk of the vehicle surface
- Bearing large design uncertainty up to 300%[1]

Afterbody Radiative Heating:

- May be important for Superorbital re-entry: Mars return
- Found to be significant with state-of-the-art simulations[2]
- No discernible data recorded by afterbody radiometers of Fire II and Apollo 4

[1] Michael J. Wright, Frank S. Milos, and Phillippe Tran. "Afterbody Aeroheating Flight Data for Planetary Probe Thermal Protection System Design". In: *Journal of Spacecraft and Rockets* 43.5 (Sept. 2006), pp. 929–943.

[2] Christopher O. Johnston and Aaron M. Brandis. "Features of Afterbody Radiative Heating for Earth Entry". In: *Journal of Spacecraft and Rockets* 52.1 (2015), pp. 105–119.

Post-mission Analyses

- Wright et al.[3] achieved excellent agreement with Fire II forebody convective heating data, but the afterbody experimental data were a factor of two higher than the noncatalytic predictions
- Johnston and Brandis[4] re-examined the FIRE II afterbody measurements and questioned the analysis of the radiometer data. Major sources of model uncertainties for afterbody radiation were identified: the rate coefficient for the three-body electron-ion recombination reaction, the escape factors on collisional-radiative modelling, and the impact of forebody ablation.

[3] Michael Wright, Mark Loomis, and Periklis Papadopoulos. "Aerothermal Analysis of the Project Fire II Afterbody Flow". In: *Journal of Thermophysics and Heat Transfer* 17.2 (2003), pp. 240–249.

[4] Christopher O. Johnston and Aaron M. Brandis. "Features of Afterbody Radiative Heating for Earth Entry". In: *Journal of Spacecraft and Rockets* 52.1 (2015), pp. 105–119.

- Johnston and Panesi[5]: treating nitrogen atoms of different grouped electronic levels as individual species in the flow field model, coupling radiative transition rates to the species continuity equations, adopting a ray-tracing approach in radiation transport calculation and developing a nonequilibrium model for NO
- Lopez et al.[6] improved the non-Boltzmann modelling of nitrogen by adopting a state-to-state description of grouped electronic states

[5] Christopher O. Johnston and Marco Panesi. "Advancements in Afterbody Radiative Heating Simulations for Earth Entry". In: *46th AIAA Thermophysics Conference*. AIAA Aviation. American Institute of Aeronautics and Astronautics, June 13, 2016.

[6] Bruno Lopez, Christopher O. Johnston, and Marco Panesi. "Improved Non-Boltzmann Modeling for Nitrogen Atoms". In: *46th AIAA Thermophysics Conference*. AIAA Aviation. American Institute of Aeronautics and Astronautics, June 10, 2016.

- West et al.[7] performed sensitivity analysis and uncertainty quantification of afterbody radiation for Stardust at peak afterbody radiative heating conditions. Four variables were found to contribute to nearly 95% of the uncertainty: the electronic-impact excitation rate for N between levels 2 and 5 and the rates of three chemical reactions that affect the number densities of N, N^+, O and O^+.
- Validation data of afterbody radiation is in high demand, particularly in the VUV wavelength range

[7] Thomas K. West IV, Christopher O. Johnston, and Serhat Hosder. "Uncertainty and Sensitivity Analysis of Afterbody Radiative Heating Predictions for Earth Entry". In: *54th AIAA Aerospace Sciences Meeting*. AIAA SciTech. American Institute of Aeronautics and Astronautics, Jan. 2, 2016.

Outline

Facility, Model and Flow Conditions

X2 Expansion Tunnel

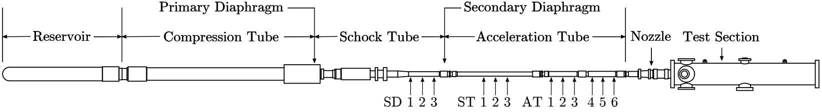

Test Model:

- 54° wedge: 25mm tall and 100 mm wide

Flow Conditions:

Condition	Velocity (m/s)	Static Pressure (Pa)	Static Temperature (K)	Stagnation Enthalpy (MJ/kg)
1	9714±0.6%	1308±8.8%	2609±1.1%	50.7±0.9%
2	10899±0.3%	1523±6.8%	2713±1.0%	63.4±0.7%
3	11837±1.0%	843±10%	2892±0.8%	75.4±2.0%

The Spectral Measurements

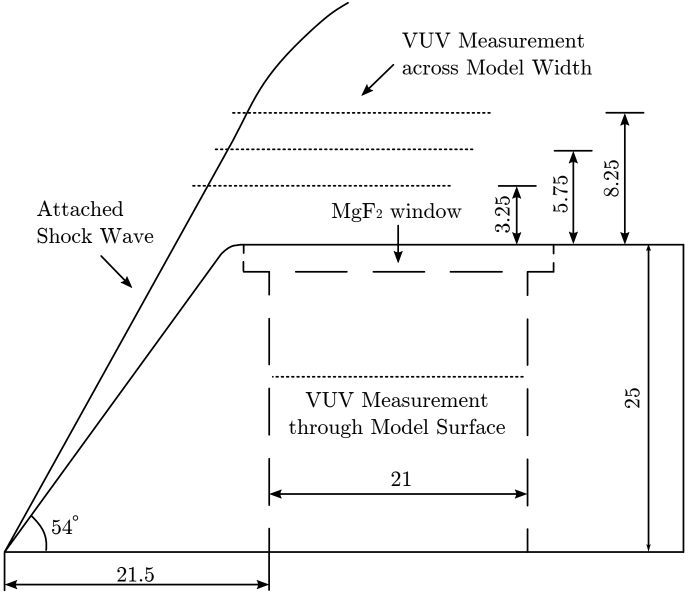

Aross-Wedge Measurement

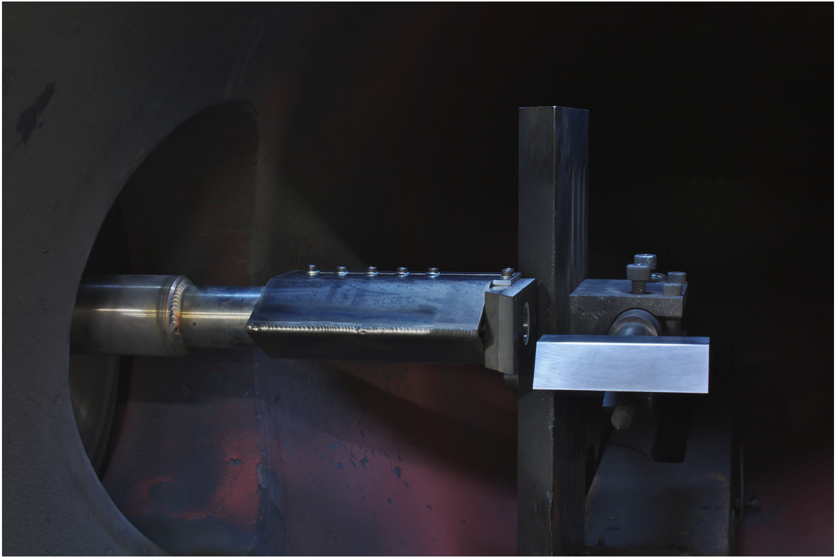

Through-Wedge Measurement

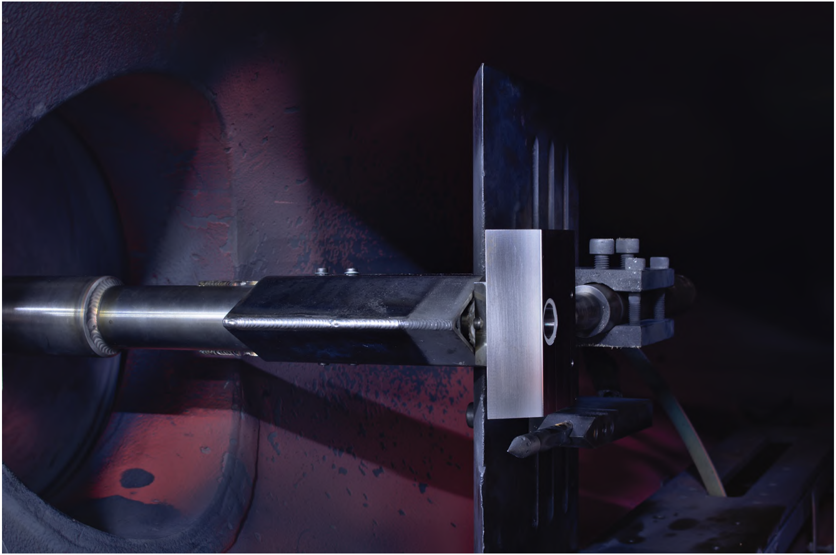

Optics Layout

- Filtered high speed imaging with a bandpass filter coupled to Shimadzu HPV-1 1MHz high speed camera (left)
- VUV emission spectroscopy system (right)

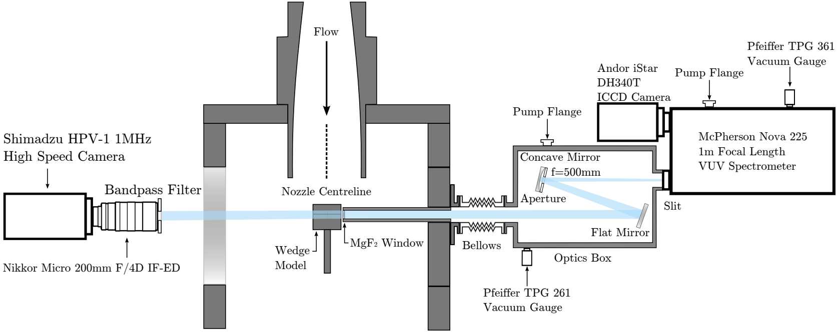

Outline

Numerical Simulation

- Flow Solver: Eilmer3[8]
- Grid Generator: GridPro
- Radiation Modelling: NEQAIR V14[9]
- Chemical Species: 11 species air including N, N^+, NO, NO^+, N_2, ${N_2}^+$, O, O^+, O_2, ${O_2}^+$ and e^-
- Thermo-chemical model: Park's two temperature model and associated reaction rates[10] with with rate controlling temperature defined as $T_d = T_{tr}^{0.7} T_{ve}^{0.3}$

[8] R. J. Gollan and P. A. Jacobs. "About the formulation, verification and validation of the hypersonic flow solver Eilmer". In: *International Journal for Numerical Methods in Fluids* 73.1 (Sept. 2013), pp. 19–57.

[9] Aaron Michael Brandis and Brett A Cruden. "NEQAIRv14. 0 Release Notes: Nonequilibrium and Equilibrium Radiative Transport Spectra Program". 2014.

[10] Chul Park. "Review of chemical-kinetic problems of future NASA missions. I - Earth entries". In: *Journal of Thermophysics and Heat Transfer* 7.3 (Sept. 1993), pp. 385–398.

Grid topology and boundary conditions

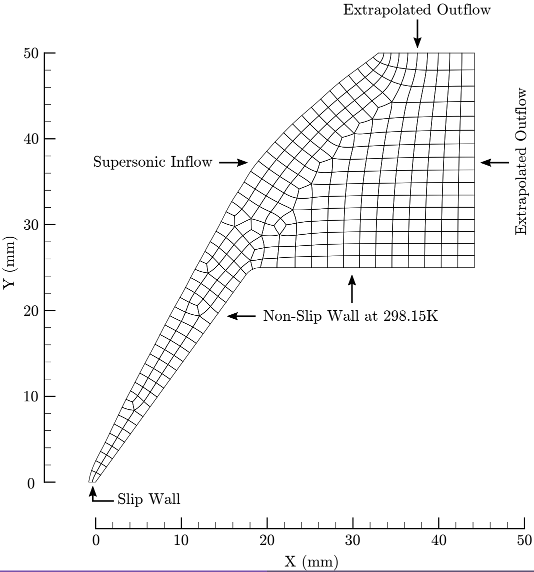

Outline

Outline

Flow Establishment

High speed video through Thorlabs FBH780-10 bandpass filter at 0.5 MHz

Flow Establishment

Synchronisation of under-model probe pressure, trigger signals and camera outputs

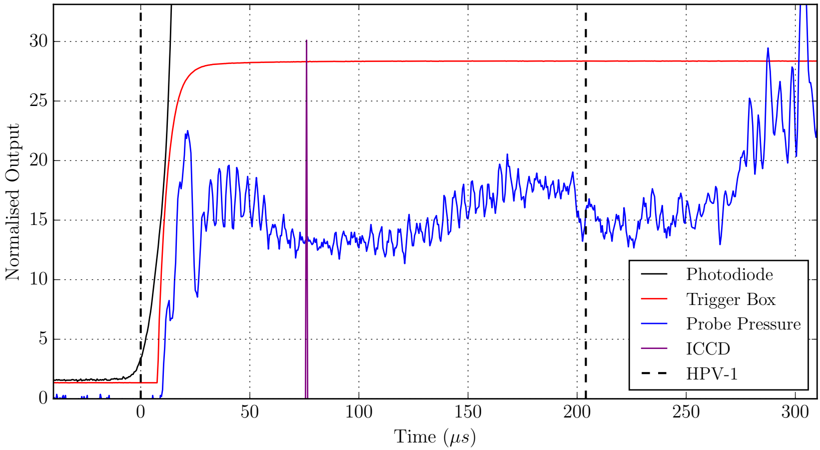

Flow Steadiness

Extracted pixel counts at 3.25mm above wedge top for Shot x2s3022 with Condition 3

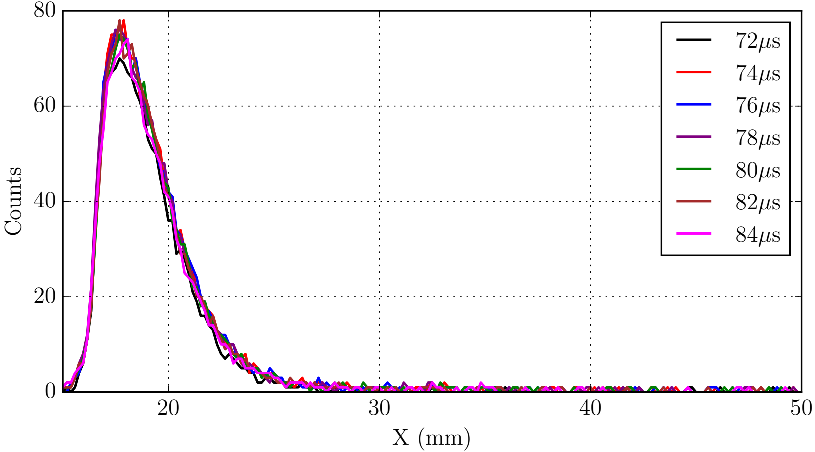

Raw spectral image for Shot x2s3022 with Condition 3

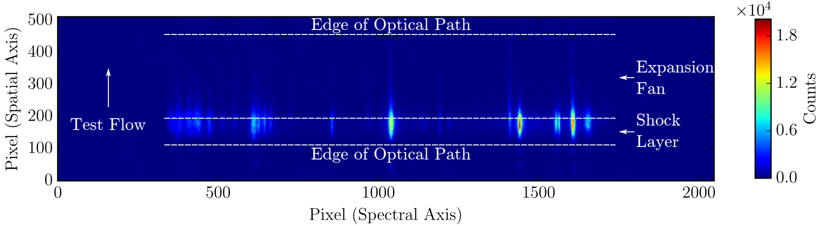

Calibrated Spectra

Calibrated spectral image for Shot x2s3022 with Condition 3

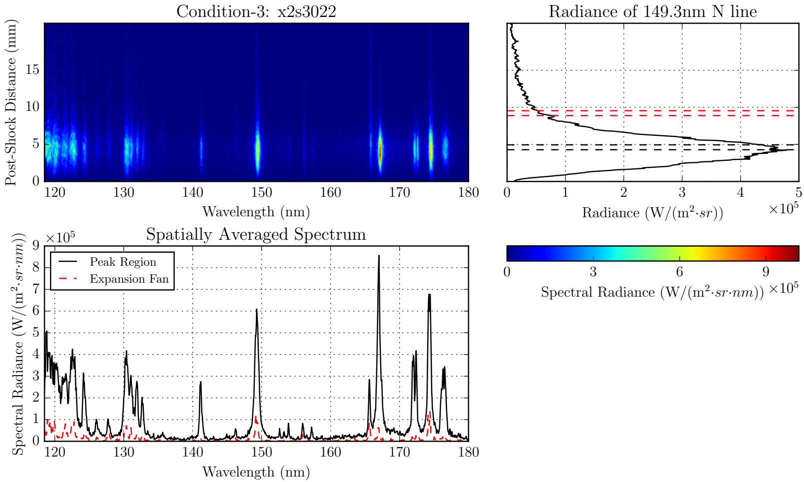

Radiator Identification

Shock layer radiators for Shot x2s3026 with Condition 1

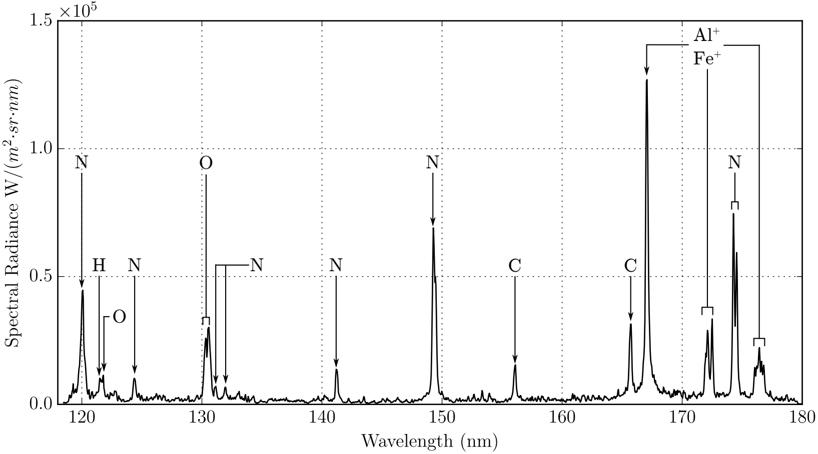

Radiator Identification

Expansion fan radiators for Shot x2s3026 with Condition 1

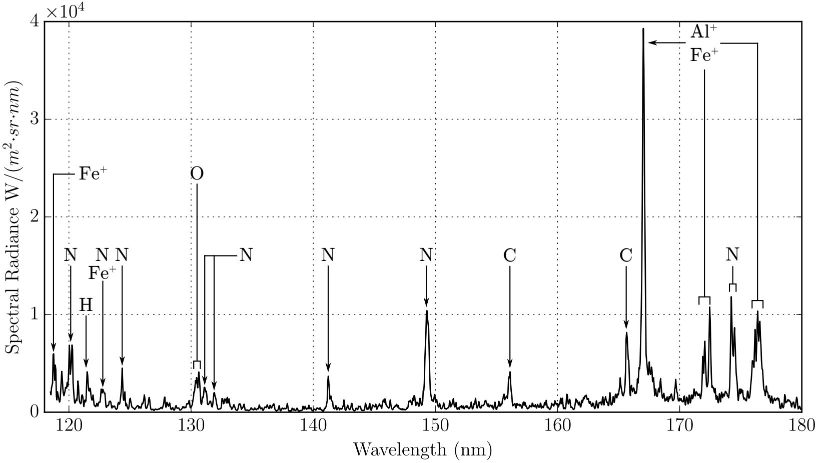

Shock layer radiators for Shot x2s3028 with Condition 2

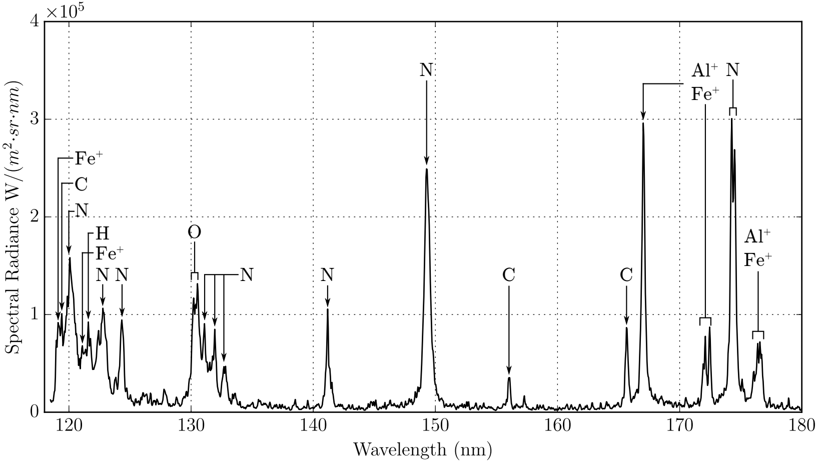

Expansion fan radiators for Shot x2s3028 with Condition 2

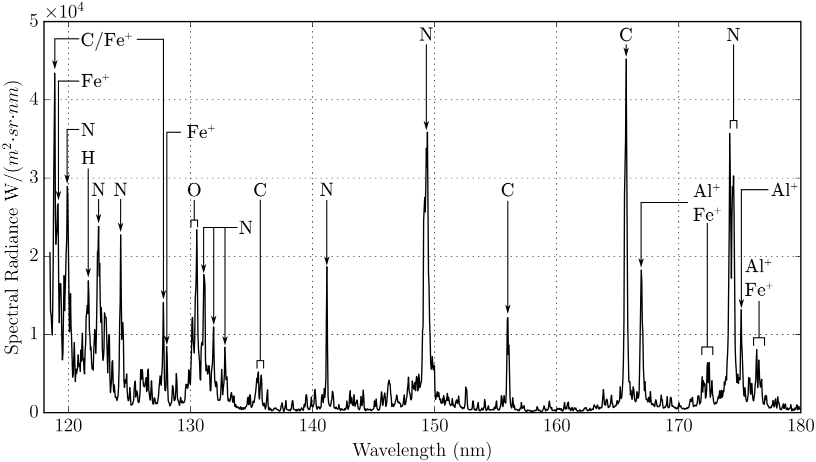

Shock layer radiators for Shot x2s3022 with Condition 3

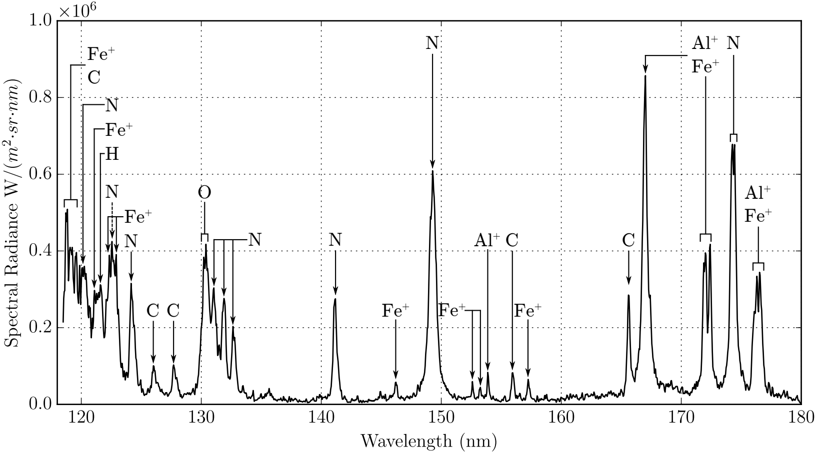

Radiator Identification

Expansion fan radiators for Shot x2s3022 with Condition 3

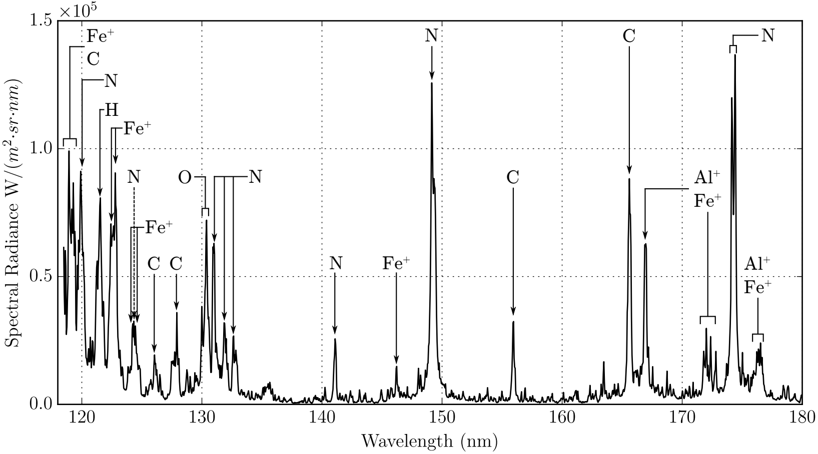

Radiator Identification

- The level of contamination increases with flow enthalpy
- The expansion fan spectra tend to be packed with more distinguishable features of contaminants
- C and Al^+ can be stronger relative to N lines in the expansion fan for certain conditions

Through-wedge spectrum of Shot x2s3056 with Condition 1

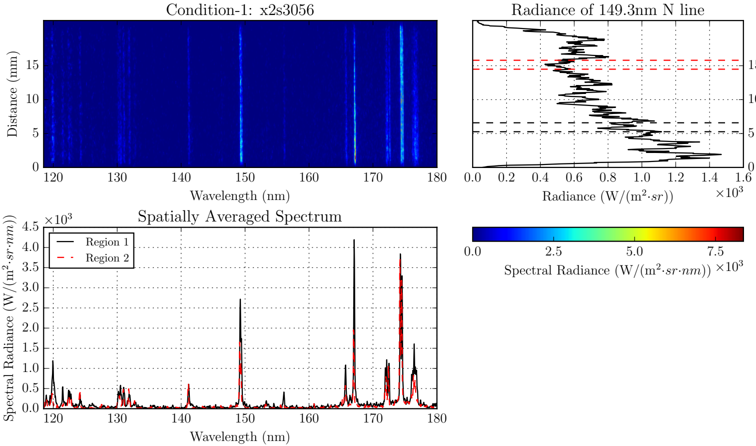

Through-Wedge Spectra

Through-wedge spectrum of Shot x2s3059 with Condition 2

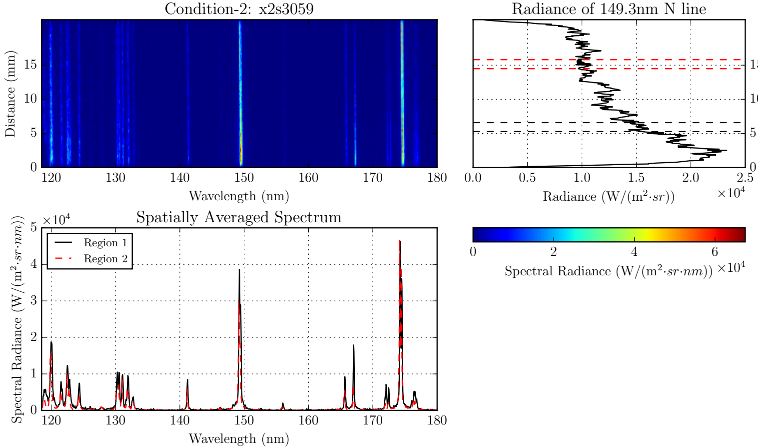

Through-wedge spectrum of Shot x2s3060 with Condition 3

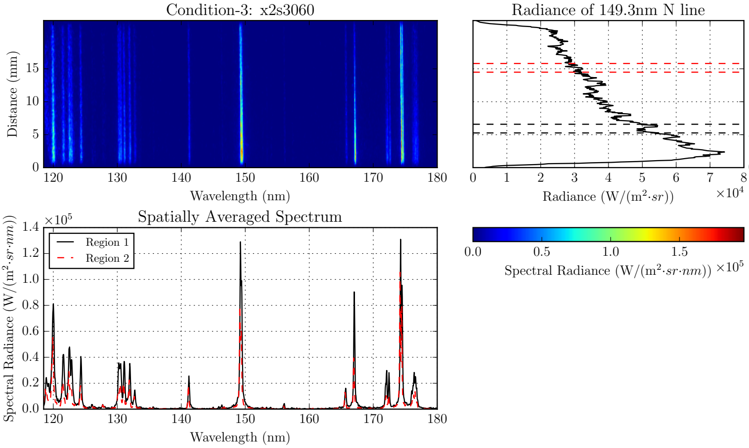

VUV Spectra vs Simulations

Radiance profiles of the 149 nm N line at 3.25, 5.75 and 8.25 mm above the top of the wedge compared between experiments and NEQAIR simulations for Condition 1

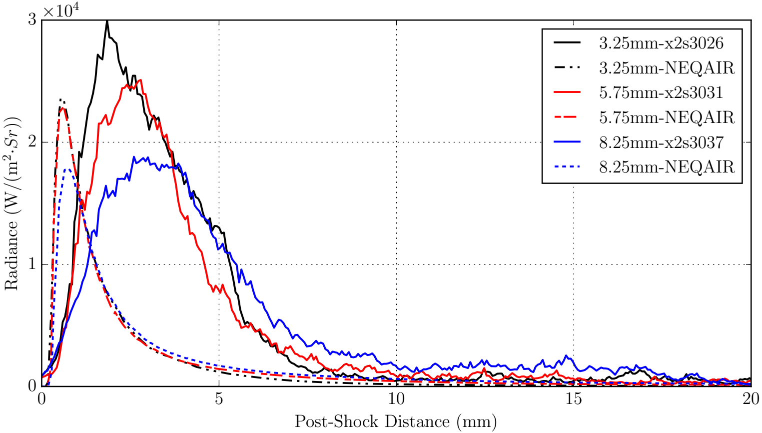

VUV Spectra vs Simulations

Radiance profiles of the 174 nm N line at 3.25, 5.75 and 8.25 mm above the top of the wedge compared between experiments and NEQAIR simulations for Condition 1

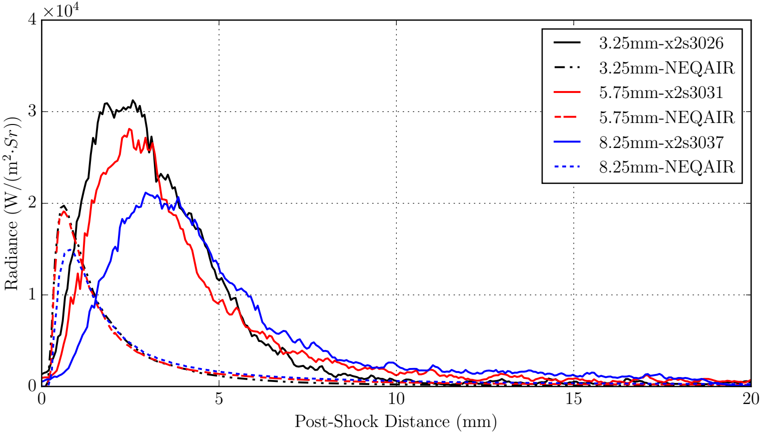

VUV Spectra vs Simulations

Experiment and NEQAIR results of the 149 nm N line, as well as selected flow variables along the line of sight at 8.25 mm above the top of the wedge for Condition 1

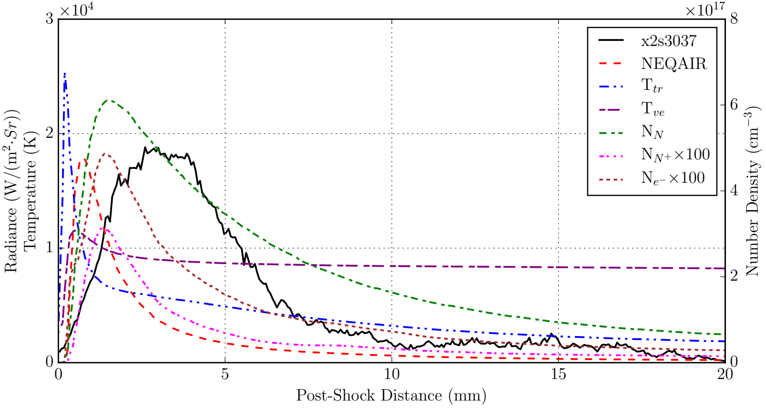

Experiment and NEQAIR results of the 149 nm N line, as well as selected flow variables along the line of sight at 8.25 mm above the top of the wedge for Condition 1

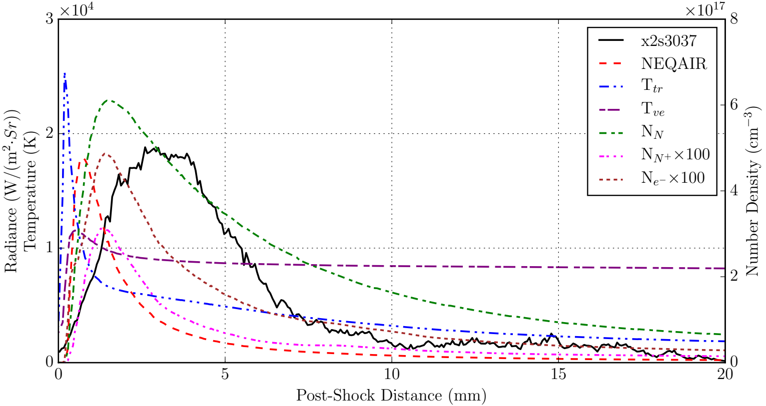

VUV Spectra vs Simulations

Density and selected species mass fraction distributions along the line of sight at 8.25 mm above the top of the wedge for Condition 1

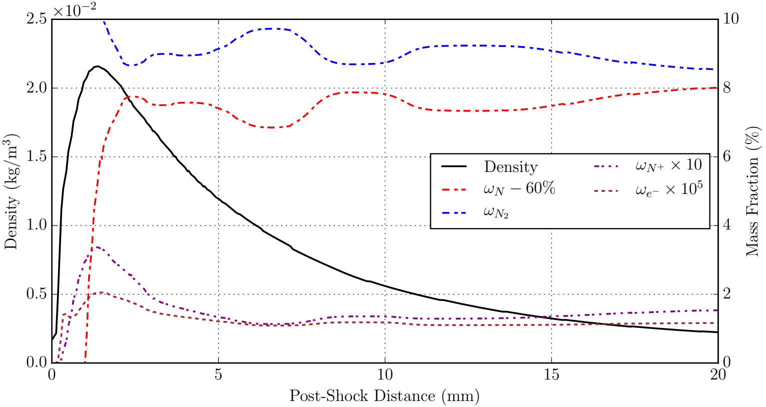

Radiance profiles of the 149 nm N line at 3.25, 5.75 and 8.25 mm above the top of the wedge compared between experiments and NEQAIR simulations for Condition 2

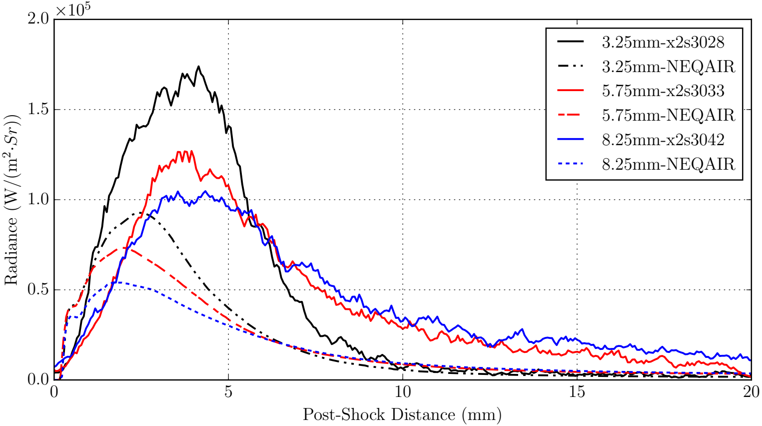

Experiment and NEQAIR results of the 149 nm N line, as well as selected flow variables along the line of sight at 8.25 mm above the top of the wedge for Condition 2

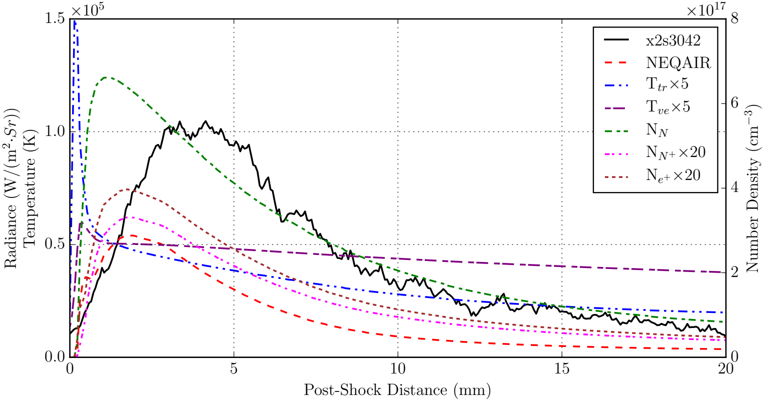

VUV Spectra vs Simulations

Density and selected species mass fraction distributions along the line of sight at 8.25 mm above the top of the wedge for Condition 2

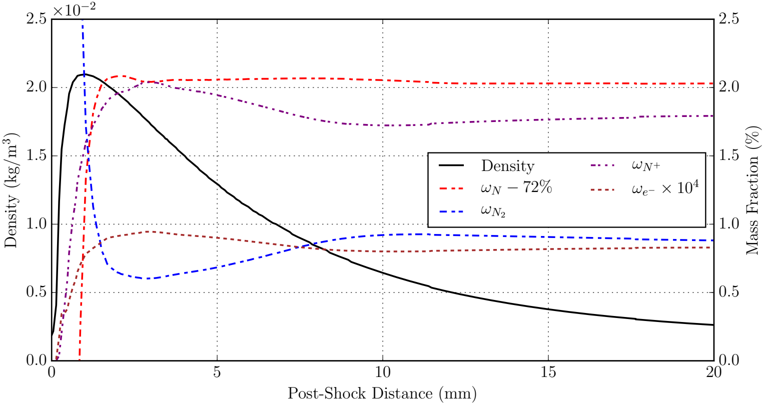

VUV Spectra vs Simulations

Radiance profiles of the 149 nm N line at 3.25, 5.75 and 8.25 mm above the top of the wedge compared between experiments and NEQAIR simulations for Condition 3

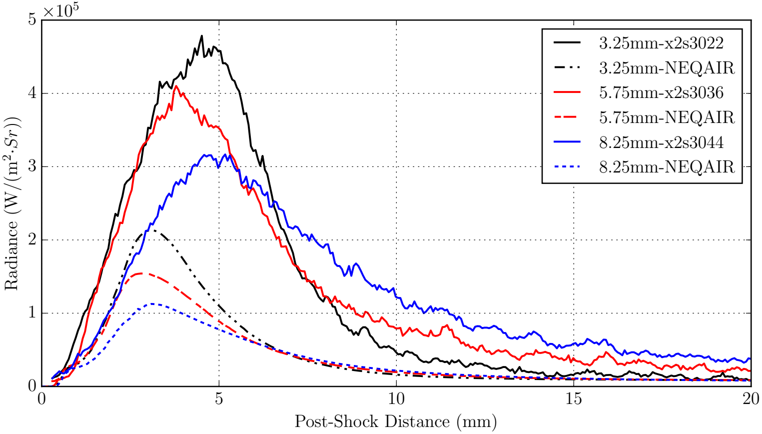

Experiment and NEQAIR results of the 149 nm N line, as well as selected flow variables along the line of sight at 8.25 mm above the top of the wedge for Condition 3

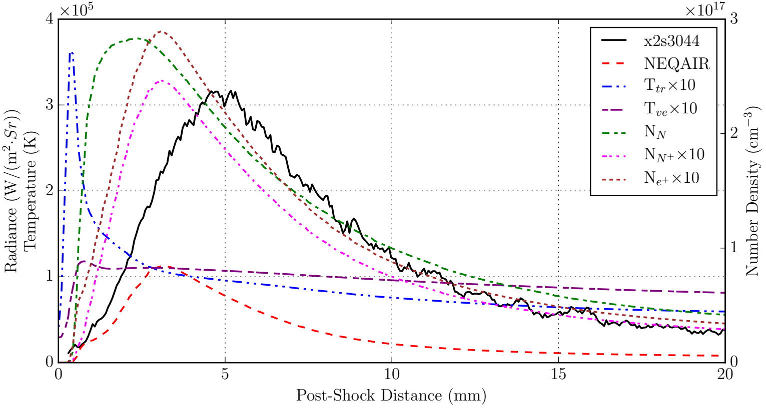

Density and selected species mass fraction distributions along the line of sight at 8.25 mm above the top of the wedge for Condition 3

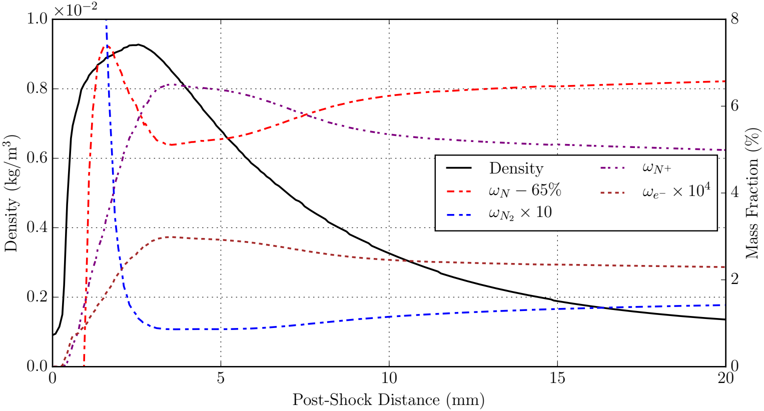

Radiance profiles of the 777 nm oxygen triplet at 3.25, 5.75 and 8.25 mm above the top of the wedge compared between experiments and NEQAIR simulations for Condition 2

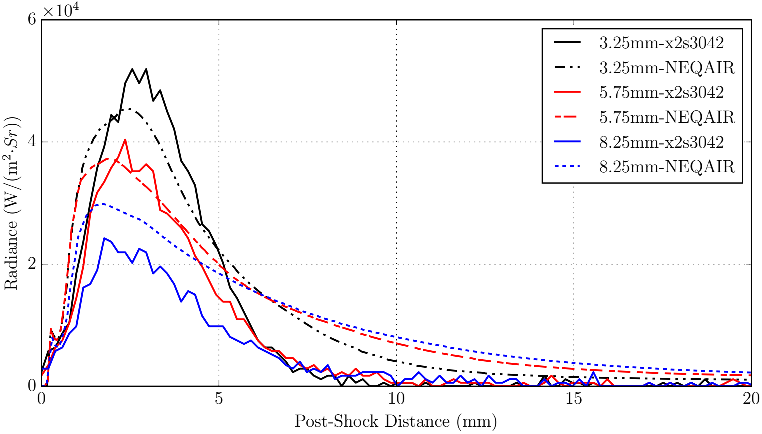

Density and selected species mass fraction distributions along the line of sight at 8.25 mm above the top of the wedge for Condition 2

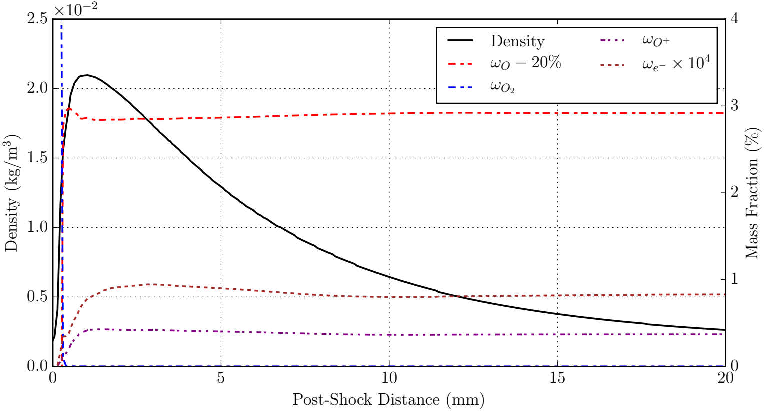

Radiance profiles of the 777 nm oxygen triplet at 3.25, 5.75 and 8.25 mm above the top of the wedge compared between experiments and NEQAIR simulations for Condition 3

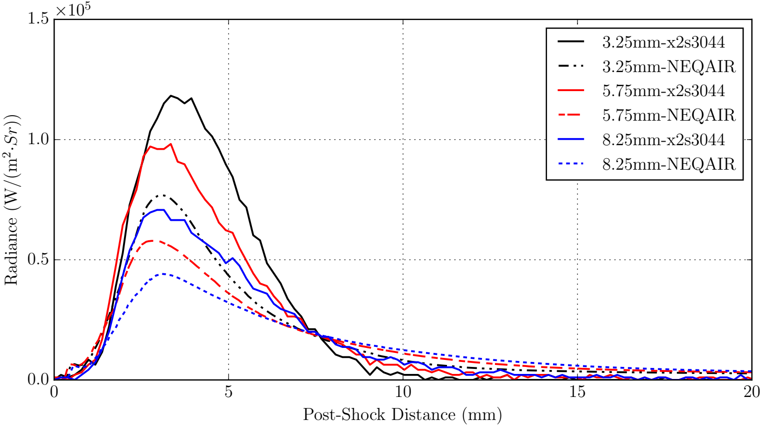

Density and selected species mass fraction distributions along the line of sight at 8.25 mm above the top of the wedge for Condition 3

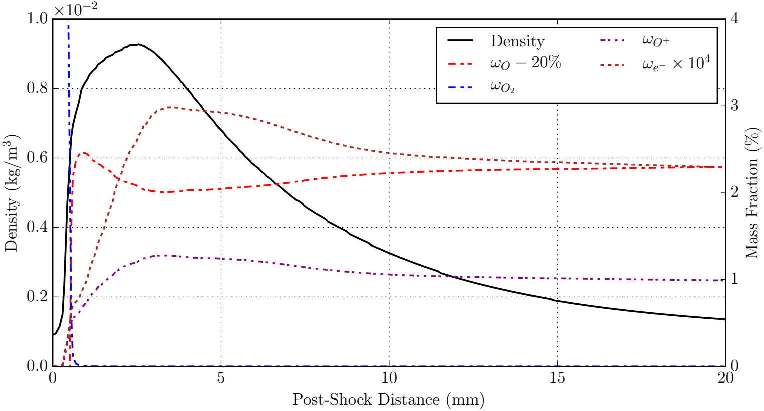

Outline

Conclusions

- The spatial profiles of 149 and 174nm N radiance are in general of larger spans than those predicted by NEQAIR
- For Conditions 2 and 3, the peak radiance levels are significantly underestimated. Large departures of predicted radiance values from experiment appear to occur at the start of the expansion fan where the electron-ion recombination process commences
- NEQAIR results agree well with the filtered images of 777nm oxygen triplet in the compression region and at the start of the expansion fan for Condition 2. For Condition 3, radiance in the compression region and at the start of the expansion fan are underpredicted by as much as 40%, but the afterbody radiance is overpredicted by up to 100%

Many Thanks

Any Questions?